Journal of Power Sources 269 (2014) 912–919

Contents lists available at ScienceDirect

Journal of Power Sources

journal homepage: www.elsevier.com/locate/jpowsour

Anode microstructures from high-energy and high-power lithium-ion cylindrical cells obtained by X-ray nano-tomography

Moses Ender*, Jochen Joos, André Weber, Ellen Ivers-Tiffée

Karlsruhe Institute of Technology (KIT), Institut für Werkstoffe der Elektrotechnik (IWE), Adenauerring 20b, 76131 Karlsruhe, Germany

HIGHLIGHTS

- Graphite anodes from power and energy cells are characterized by HR X-ray nano-CT.
- Microstructure quantification by calculating characteristic structural parameters.
- First direct comparison of microstructures from a high-energy and a high-power cell.
- Discussion of differences in the microstructures and the effects on performance.
- Ion transport in the pores limits performance of the energy cell anode.

ARTICLE INFO

Article history:
Received 6 May 2014
Received in revised form
19 June 2014
Accepted 9 July 2014
Available online 22 July 2014

Keywords:
Lithium-ion
Negative electrode
Microstructure
High-energy
High-power
X-ray tomography

ABSTRACT

Graphite negative electrodes from a high-power and a high-energy cylindrical lithium-ion cell are reconstructed using X-ray nano-tomography. Large volumes and high resolution are required for an in-depth comparison of the design aspects for high-power and high-energy anode. Hence, quite big volumes of $2.37 \cdot 10^6$ μm^3 and $1.27 \cdot 10^6$ μm^3 have to be analyzed to cover the entire thickness of both anode layers. High resolutions of 273 nm and 233 nm voxel size are chosen for assessing volume specific graphite surface area, among other parameters, precisely. A hysteresis segmentation method is adapted for segmentation, featuring a symmetrical growing of both graphite and pore phase. Surface areas are calculated using the marching cube algorithm, particle sizes are calculated based on the Euclidean distance transform (EDT) and tortuosity values are calculated by solving the transport equation using a finite volume scheme in MATLAB. Analysis of these parameters leads to the assumption, that the electrolyte transport is limited by the pore structure of the high-energy graphite anode.

1. Introduction

The lithium-ion cells in today's state-of-the-art applications are optimized for their intended use which can be classified by two basic categories. First, this are applications which require high energy content such as mobile electronic devices (cell phones, tablet pcs and laptops), where a long-lasting battery operation is demanded. Second, this are applications with a high power consumption such as power tools (e.g. cordless screwdriver), requiring a high power for a limited time. Therefore, lithium-ion cells can be categorized in (a) high-power cells and (b) high-energy cells.

The chemistry of the active material is only one possible difference between these two types of lithium-ion cells. Especially for the anodes (negative electrodes), graphitic carbon is used as anode active material in almost all cells. The difference between a graphite anode of a high-power cell and of a high-energy cell must therefore be found in the electrode microstructure characteristics. It is of common knowledge, that particle and/or agglomerate size as well as porosity and layer thickness should be custom-tailored for both types of anodes, but numerical values of (I) volume fractions, (II) tortuosity, (III) surface areas and (IV) particle sizes have not been accessible so far.

There are basically two methods applicable to reconstruct the electrode microstructure of a porous electrode: focused ion beam (FIB) tomography and X-ray tomography [1–4]. Active material, carbon black and pore phase of a $LiFePO_4$-cathode, well-designed for high-power, was already reconstructed using FIB tomography. Microstructural features such as agglomerates differing in particle size and porosity, three-dimensional distribution of carbon fibers

Abbreviations: CT, computed tomography; EDT, Euclidean distance transform; EMC, ethyl methyl carbonate; FIB, focused ion beam; $LiCoO_2$, lithium cobalt oxide; $LiFePO_4$, lithium iron phosphate; SEM, scanning electron microscope.

* Corresponding author. Tel.: +49 721 6084 7599; fax: +49 721 608 4 74 92.
E-mail address: moses.ender@kit.edu (M. Ender).

http://dx.doi.org/10.1016/j.jpowsour.2014.07.070
0378-7753/

for electron transport, and surface area accessible by electrolyte were reported in a previous work of our group [5]. But, as the average particle size of graphite anodes is approximately ten times larger, X-ray nano-tomography is the method of choice. Hence, volumes of $2.37 \cdot 10^6$ μm^3 and $1.27 \cdot 10^6$ μm^3 were analyzed in this work, large enough for being representative volume elements [6]. High resolutions of 273 nm and 233 nm voxel size were chosen, enabling an assessment of surface areas of graphite particles, accessible by the liquid electrolyte.

The investigated cells were state-of-the-art cylindrical cells with cell A denoting the high-power cell and cell B denoting the high-energy cell (Table 1).

2. Graphite negative electrodes and preparation

The high-power 18650 cell (cell A) in Table 1 was made of a $LiFePO_4$ cathode and a graphite anode, the high-energy 18500 cell (cell B) was made of $LiCoO_2$ and graphite. Both cell types were opened in an Argon filled glove box, the graphite anodes were rinsed with ethyl methyl carbonate (EMC) for removal of electrolyte and stored in a vacuum chamber to evaporate the EMC. The microstructure characteristics of both graphite anodes, denoted as anode A and anode B, were analyzed by scanning electron microscopy (SEM). SEM images of the surface, after removal of electrolyte and EMC, are shown in Fig. 1. There is no information available about the exact composition of the electrodes or about the properties of the used powders. As indicated by the characteristic shape of the open circuit potentials shown in Fig. 2, both anodes possess a graphitic structure. The minor differences in the shape of the different stages suggest a difference in the microscopic structure, e.g. crystallite size.

The SEM micrographs do not reveal specific features that are different between both anodes. Both consist of particles of irregular shape with sizes up to 20 μm, which are randomly arranged. In addition to the graphite particles, anode A shows some carbon fibers which are added to better connect the graphite particles. A difference in porosity, which might be expected, is not detectable. The similar appearing in SEM micrographs underlines the necessity of a three-dimensional reconstruction by tomography methods. As a next step, both anodes were prepared for X-ray tomography. For this purpose, the copper current collector had to be removed, as copper has a strong absorption coefficient at low X-ray energies. This was done by dipping the electrode into diluted hydrochloric acid (18%) for about 10 s, after which the coating was detached from the current collector. The porous graphite layer was then rinsed with distilled water and dried over night at 60 °C. After this treatment, the structural integrity of samples from anode A and anode B was ensured by SEM inspection. For anode A, both sides of the obtained porous graphite layer are shown in Fig. 3. The surface of anode A, which was directed towards the separator (Fig. 3a), has still the same appearance as in Fig. 1a. The opposite surface shown in Fig. 3b, formerly attached to the current collector, still shows the irregular binder network. This proves that the binder is not affected by exposing the electrode to diluted hydrochloric acid, thus the binding forces between the individual graphite particles are still intact.

Table 1
Lithium-ion cells with high-power and high-energy characteristics.

	Cell A (high-power cell)	Cell B (high-energy cell)
Cell chemistry	$LiFePO_4$/graphite	$LiCoO_2$/graphite
Nominal capacity	1.1 Ah	1.5 Ah
Energy content	3.52 Wh	5.1 Wh
Mass	38.8 g	35 g
Maximum specific power	1800 W kg^{-1}	290 W kg^{-1}
Maximum specific energy	90.7 Wh kg^{-1}	158 Wh kg^{-1}
Anode thickness	47.7 μm	76.1 μm

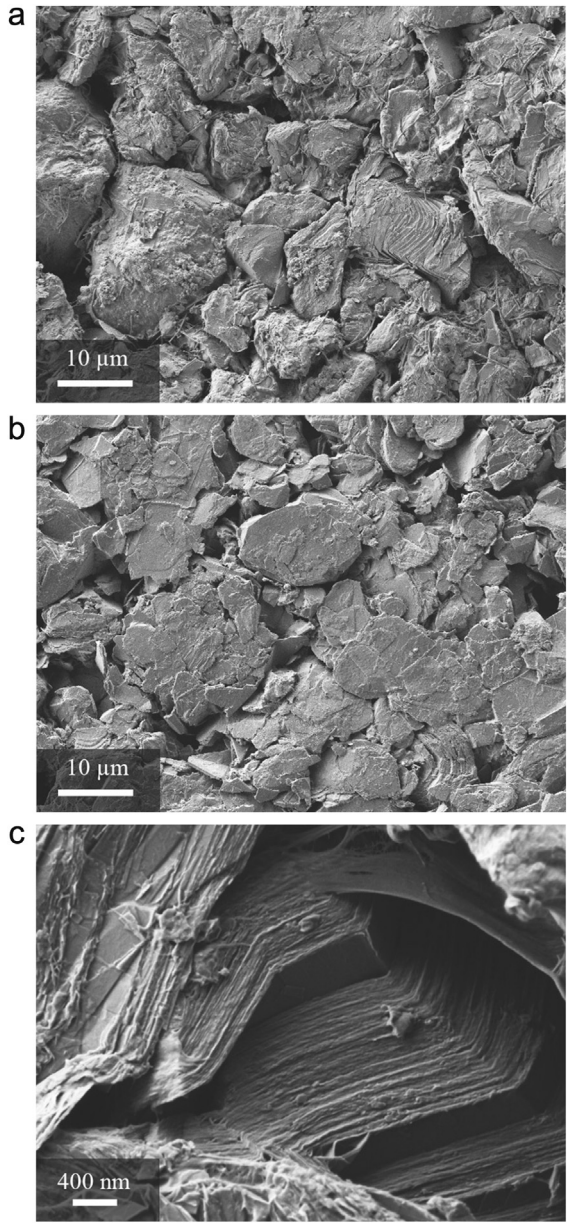

Fig. 1. SEM micrographs of the graphite anodes from (a) the high power cell (anode A from cell A) and (b) of the high energy cell (anode B from cell B). Additionally, a high-resolution image of the anode A is given (c), showing the slaty structure of a graphite particle edge.

3. Reconstruction and segmentation

The porous graphite layers, which were detached from the current collector, were used for the actual X-ray computed tomography (CT). To mount the samples at the sample holder, they were further subdivided and suitable pieces were selected. The scan was done with a Bruker nano-CT SKYSCAN 2011 with a source voltage of 30 kV for anode A and 40 kV for anode B. Recording and reconstruction of the projection images was performed by our partner RJL Micro & Analytic GmbH (http://www.rjl-microanalytic.de). Cross-sections of the raw data from both anodes are shown in Fig. 4 and the properties of the reconstruction datasets are listed in